Title

Priming Chondrocytes During Expansion Alters Cell Behavior and Improves Matrix Production in 3D Culture

Authors

Lindberg, Emily D
Wu, Tiffany
Cotner, Kristen L
et al.

Publication Date

2023-12-01

DOI

10.1016/j.joca.2023.12.006

Priming Chondrocytes During Expansion Alters Cell Behavior and Improves Matrix Production in 3D Culture

Emily D. Lindberg[1]

Tiffany Wu[2]

Kristen L. Cotner[3]

Amanda Glazer[4]

Amir A. Jamali[5]

Lydia L. Sohn[1,3]

Tamara Alliston[6]

Grace D. O'Connell[1,6]

[1] Department of Mechanical Engineering
University of California, Berkeley, USA

[2] Department of Bioengineering
University of California, Berkeley, USA

[3] UC Berkeley-UCSF Graduate Program in Bioengineering
University of California, Berkeley, USA

[4] Department of Statistics
University of California, Berkeley, USA

[5] Joint Preservation Institute
Walnut Creek, CA

[6] Department of Orthopedic Surgery
University of California, San Francisco, USA

Submitted to: Osteoarthritis and Cartilage
Running title: *Priming alters cell behavior and matrix production*
Corresponding Author: Grace D. O'Connell
5122 Etcheverry Hall, #1740,
Berkeley, CA, 94720-1740
e-mail: g.oconnell@berkeley.edu

Abstract

Objective: Cartilage tissue engineering strategies that use autologous chondrocytes require *in vitro* expansion of cells to obtain enough cells to produce functional engineered tissue. However, chondrocytes dedifferentiate during expansion culture, limiting their ability to produce chondrogenic tissue and their utility for cell-based cartilage repair strategies. The current study identified conditions that favor cartilage production and the mechanobiological mechanisms responsible for these benefits.

Design: Chondrocytes were isolated from juvenile bovine knee joints and cultured with (primed) or without (unprimed) a growth factor cocktail. Gene expression, cell morphology, cell adhesion, cytoskeletal protein distribution, and cell mechanics were assessed. Following passage 5, cells were embedded into agarose hydrogels to evaluate functional properties of engineered cartilage.

Results: Priming cells during expansion culture altered cell phenotype and chondrogenic tissue production. Unbiased RNA-sequencing analysis suggested, and experimental studies confirmed, that growth factor priming delays dedifferentiation associated changes in cell adhesion and cytoskeletal organization. Priming also overrode mechanobiological pathways to prevent chondrocytes from remodeling their cytoskeleton to accommodate the stiff, monolayer microenvironment. Passage 1 primed cells deformed less and had lower YAP1 activity than unprimed cells. Differences in cell adhesion, morphology, and cell mechanics between primed and unprimed cells were mitigated by passage 5.

Conclusions: Priming suppresses mechanobiologic cytoskeletal remodeling to prevent chondrocyte dedifferentiation, resulting in more cartilage-like tissue-engineered constructs.

Key words: chondrocyte dedifferentiation, cartilage tissue engineering, cell adhesion, cartilage regeneration

Introduction

Articular cartilage has a limited self-healing capability from trauma or degenerative diseases, such as osteoarthritis (OA), resulting in joint pain and dysfunction. OA is the most common joint disease worldwide, affecting over 30 million adults in the United States[1]. Due to an aging population and an increase in younger patients (<60 years of age) developing cartilage defects[2], there has been a shift towards using tissue engineering strategies to repair smaller, early-stage cartilage lesions to restore joint biomechanics and prevent further damage.

There have been significant advancements in the development of biological repair strategies, such as matrix-induced autologous chondrocyte implantation (MACI), that aim to overcome cartilage's inability to regenerate by engineering tissue-scaffolds *in vitro* and implanting them directly into cartilage defects[3]. Although these techniques have shown promise, the engineered cartilage substitutes produced do not possess the same mechanical and biochemical properties as native articular cartilage, which may subsequently reduce implant longevity[4]. Chondrocyte dedifferentiation during monolayer expansion (i.e., two-dimensional, 2D) culture is responsible for the inferior quality of cartilage tissue substitutes[5]. Dedifferentiated chondrocytes experience a phenotypical and morphological shift towards fibroblast-like cells, resulting in a decreased ability to produce extracellular matrix (ECM) rich in collagen type II and aggrecan upon transfer to three-dimensional (3D) culture[6-8].

Cells are highly influenced by their surrounding microenvironment, with factors including substrate stiffness[9-11], cell density, media osmolarity, gas concentration, and exogenous growth

factors[12, 13] affecting gene expression and protein production. Specifically, priming cells with a combination of TGF-β1, FGF2, and PDGF-ββ during 2D expansion culture has been effective in increasing chondrogenic matrix production in 3D culture. This technique has been used to create engineered cartilage with chondrocytes obtained from healthy adult canine joints[14], juvenile bovine joints[15], and both healthy and osteoarthritic human cartilage[16, 17]. Despite promising results, the mechanisms underlying the long-term effects of priming during 2D expansion on 3D tissue production remain poorly understood, and the presence of specific biomarkers that could predict successful development of cartilage-like tissue is yet to be determined.

Thus, the objective of this study was to determine the relationship between cell properties during 2D expansion culture and 3D matrix production. Specifically, we investigated how growth factor priming during expansion culture alters cell phenotype and improves chondrogenic matrix production. Findings from this study provide valuable insights into cell characteristics that may be important for identifying and expanding autologous chondrocytes that can successfully recapitulate healthy functional cartilage.

Materials and Methods

Study Design

Chondrocytes were isolated from juvenile bovine knee joints and cultured in media with (primed, +GF) or without (unprimed, -GF) a growth factor cocktail consisting of 1ng/mL TGF-β1, 10ng/mL PGDF-ββ, and 5ng/mL FGF-2 for up to passage 5 (Figure 1). The effect of priming on gene expression, cytoskeletal distribution, cell adhesion, and single-cell mechanics were evaluated following passage 1, 3, and 5. Analyses were performed to assess how cellular changes due to

priming translated to differences in tissue mechanics and biochemical composition in 3D culture. For extended methods please see supplemental material.

RNA expression analysis

Total RNA was isolated from unprimed and primed chondrocytes from each condition and sent to UCSF Genomics Core Facility for RNA-sequencing and data processing (n=3 wells/group). Differential expression was performed to determine pairwise combinations with respect to expansion culture condition (primed to unprimed). Differentially expressed genes (DEGs) with a false discovery rate (FDR) value <0.01 were considered significant. Gene ontology enrichment analysis of DEGs upregulated and downregulated due to priming (FDR<0.01) were analyzed separately using DAVID Bioinformatics Database. Categories with a Benjamini-Hochberg adjusted p-value < 0.05 were considered significant. Gene ratios were calculated for each enriched gene ontology term. Ingenuity Pathway Analysis (IPA) software was used to further analyze DEGs. The right-tailed Fisher's exact test (p<0.01) was used to calculate statistical significance and the z-score was used to identify the observed activation state (z-score≥2 for activated and ≤-2 for inhibited). RNA-seq was validated with qPCR (Supplemental Table 1). Reactions (n=3 wells/ group) were run in duplicate, followed by quantification using the $\Delta\Delta C_t$ method with normalization to *GAPDH*.

Mechanical characterization of single cells

A custom-built microfluidic device with a microfluidic contraction channel embedded in polydimethylsiloxane (PDMS) was fabricated using standard soft-lithography and used to determine cell stiffness[18]. The device included a contraction channel that applied a compressive strain to cells as it traversed through the channel. A non-pulsatile inlet pressure was applied to flow cells through the channel, and a constant DC voltage was applied to measure current pulses

caused by cells as they transited the device. Current data was filtered using a low-pass filter, and a custom written software (https://github.com/sohnlab/NPS-analysis-chondrocytes) was used to calculate the magnitude and duration of each current sub-pulse. Each group was tested in triplicate using three different devices. Deformed diameter and transverse deformation were calculated based on a constant strain applied to cells (target strain range = 0.1-0.4) within the contraction channel based on methods described in Kim *et al.*[18]. To account for differences in cell size, preliminary experiments were performed to determine the expected cell diameter and devices were fabricated with contraction channels of two sizes (9.8 and 10.5um) to achieve the target applied strain range for each passage and experimental group. One- to-one matching was used to ensure no significant difference in strains between primed and unprimed cells. After matching, two-sided permutation tests were used to compare unprimed and primed cells at each passage and evaluate the effect of passaging on transverse deformation (n=3 devices/group; >68 cells/group).

Immunofluorescence

48 hours after plating, cells were prepared for immunostaining of actin fibers and focal adhesions. First, cells were incubated with a primary antibody against vinculin, followed by a one-hour incubation with an Alexa Fluor 594 secondary antibody. Cells were then stained for F-actin using Alexa Fluor 488 Phalloidin and cell nuclei using DAPI. Maximum pixel projection images were generated in ImageJ and phalloidin stained images were used to calculate cell spreading area (n=3 wells/group; 45-80 cells). F-actin images were randomized and shown to three independent graders (n=3 wells/ group; 52-79 cells). Graders classified each image in one of two groups based on stress fiber clarity in the cytoplasm (Supplemental Figure 1). Graders showed good interrater reliability, with 76% agreement (confidence interval: 72-79; κ=0.60).

To examine YAP nuclear localization, cells were cultured for 3 days, fixed, permeabilized, and blocked for non-specific binding. Cells were incubated with a mouse anti-Yap1 primary antibody, then incubated with Alexa Fluor 594 goat anti-mouse secondary antibody. DAPI was applied for nuclear staining before imaging. YAP distribution was calculated as the staining intensity in the nucleus divided by staining intensity in the cytoplasm (n=3 wells/group; 297 cells). Differences in YAP expression between P1 unprimed and primed cells was compared using an unpaired two tailed parametric t-test (p=0.006).

Cell adhesion assays

For centrifugation-based cell adhesion assays, cells were incubated in 10% serum media with 1ug/mL Hoechst and seeded into 24 well plates for 20 minutes. Cells were imaged to determine initial cell number. Wells were filled with fresh media and plates were sealed, inverted, and centrifuged at 2250g for 5 minutes. Following centrifugation, fresh media was added, and the plates were re-imaged. ImageJ was used to overlay images and count the remaining cells (3 wells/group, 3 images/well).

For the trypsin-based adhesion assay, primary and P2 cells were expanded to ~70% confluence in 24-well plates[19]. Hoechst was added to the culture media and cells were incubated for 30 minutes. Cells were imaged to determine initial cell count, washed with PBS, and then trypsin was added to all wells. At each time point, 10% serum-media was added to the appropriate wells to deactivate the trypsin. Media was changed in each well to remove any floating cells. All wells were reimaged, and remaining cells were calculated (3 wells per time point, 3 images/ well).

3D tissue culture: mechanics and biochemistry

After P5, cells were embedded in 2%/wv Type VII-A agarose and cast between two glass plates ($36.4 \pm 6.8 \times 10^6$ cells/mL). Cylindrical constructs (diameter=4mm, thickness=2.45±0.04mm) were

cultured for 35 days in serum-free chemically defined medium supplemented with 10ng/mL TGFβ3 for the first 14 days[14, 17]. Cells were also encapsulated in agarose after P3; however, those results are not presented due to an issue with nutrient diffusion (Supplemental Figure 2)[20].

Unconfined compression testing was performed to evaluate initial and final mechanical properties under stress relaxation (10% strain). Equilibrium modulus was calculated at the end of a 30-minute hold (n=8 constructs/group). After mechanical testing, wet weights (ww) were measured, and samples were lyophilized to determine dry weights (dw). Swelling ratio (SR) was calculated by normalizing day 35 ww by the average ww from day 1 for each group. Lyophilized samples were digested overnight in proteinase K. DNA, glycosaminoglycan (GAG), and hydroxyproline contents were measured (n=8/group). The mass ratio of hydroxyproline to collagen was assumed to be 7.64 and used to calculate total collagen content. GAG and collagen contents were normalized by ww and DNA content to measure matrix composition and cell activity in matrix production, respectively.

Statistical analysis

For statistics, a two-way ANOVA with factors of days in culture and priming was used to examine differences in gene counts, cell spreading area, cell adhesion, tissue mechanics, and matrix composition. Changes in cell adhesion over time was assessed with a two-way ANOVA (factors = passage and time point). A Tukey post-hoc analysis was performed whenever statistical significance was achieved ($p \leq 0.05$). Differences in tissue composition and mechanics with priming was compared using an unpaired two-tailed parametric t-test.

Results

Transcriptional profiling reveals differences based on both growth factor priming and passage number during chondrocyte monolayer expansion

Hierarchical clustering and principal component (PC) analysis indicated clear clustering of gene expression profiles based on passage and priming, with P1 primed cells showing the greatest difference from other groups (Figure 2A-2B). At higher passages, primed and unprimed cells clustered similarly along PC2, suggesting a convergence with passaging. A similar ratio of downregulated to upregulated genes occurred at all passages; however, the number of significant DEGs were nearly 2-fold greater for P3 and P5 when compared to P1, and the greatest overlap in DEGs occurred between P3 and P5 (Figure 2C-2D).

We identified three downregulated (*CDH13, CCN3, and NID1*; Figure 2E) and three upregulated (*POSTN, COL8A1, and GPRC5A*; Figure 2F) genes that were among the most significant at all passages. Genes associated with ECM function and organization were identified in the top ten most significantly expressed DEGs in unprimed cells, while highly expressed genes in primed cells related to matrix organization. RNAseq expression was compared to qRT-PCR for four chondrogenic genes[21], and consistent values were observed, ensuring accuracy of the RNAseq analysis (Figure 2G). Next, we investigated the mRNA ratio of markers of differentiated chondrocytes in hyaline cartilage to markers of dedifferentiated chondrocytes in fibrocartilage and found a significant difference in the *COL2A1/ COL1A1* and *ACAN/VCAN* ratio based on priming only at P1 (P1, p=0.0002; Figure 2H-2I).

Gene expression shows enrichment for proliferation in primed cells and cell adhesion in unprimed cells

The analysis of downregulated genes in primed cells compared to unprimed cells at all passages identified a prominent role of genes associated with cell signaling, communication, adhesion, and movement (Figure 3A). Cellular components significantly enriched for genes in unprimed were related to cellular adhesion at P1 and the matrix and vesicles at P3 and P5 (Figure 3B).

Furthermore, similar gene enrichment was identified between genes expressed in primed cells at P3 and P5, with biological processes related to the cell cycle, gene expression, RNA processing (Figure 3C) and cellular components in the nucleus (Figure 3D). These results suggest that primed cells may be in a more proliferative state compared to unprimed cells. In contrast, unprimed cells may be responding more to changes in substrate stiffness, with differentially expressed genes associated with signal transduction, cell adhesion, and movement. For completeness, differences in molecular functions with growth factor priming were also examined for each passage (Supplemental Figure 3).

Growth factor priming during monolayer expansion reduces cell-substrate adhesion

Numerous biological and cellular processes related to cell adhesion were identified as significantly enriched in DEGs downregulated with priming at all passages ($p < 0.01$; Supplemental Table 2). Therefore, we performed further analysis on significant DEGs belonging to the downregulated GO term "positive regulation of cell substrate adhesion ($p < 0.01$; Figure 4A). The greatest overlap in transcribed genes related to cell adhesion occurred at P3 and P5.

A centrifugation-based cell adhesion assay showed that priming significantly reduced cell adhesion at P1 and P3 ($p<0.0001$); however, at P5, cells remained attached to the substrate regardless of priming condition ($p=0.99$; Figure 4B). The trypsin-based adhesion assay confirmed cell adhesion results from the centrifugation-based assay, with a significantly greater percent of primed cells detaching from the substrate at both P1 (3.5-8 minutes, $p\leq0.02$; Figure 4C) and P3 (all time points, $p\leq0.02$; Figure 4D) compared to unprimed cells. Differences in cell adhesion based on passage revealed significantly more cells detaching at P1 than P3 (3.5-8 minutes, $p<0.0001$; Figure 4E) in unprimed cells and no significant difference at any time point for primed cells ($p>0.87$; Figure 4F).

Priming decreases actin stress fiber formation and cell spreading area at low passages

The greatest priming-dependent differences in cytoskeleton organization were observed at P1 (Figure 5A), where unprimed cells had defined stress fibers and focal adhesions. The relative number of cells with stress fibers increased with each passage for both unprimed and primed cells, and unprimed cells consistently contained a greater percentage of cells with stress fibers ($p<0.002$) after P0 ($p=0.99$; Figure 5B). Cell spreading followed a similar pattern as actin distribution, where unprimed cells spread rapidly between initial seeding and P1, and this response was maintained through P5 (Figure 5C). In line with observed patterns in cell adhesion, priming prevented cell spreading during early passages ($p<0.0001$); however, by P5, cell spreading area was similar between groups ($p=0.29$). IPA results showed that cell protrusion formation, filament formation, and cytoskeleton organization were enhanced in unprimed cells at all passages (Figure 5D).

Growth factor priming influences YAP1 signaling in passage 1 cells.

QIAGEN IPA upstream regulator function identified transcriptional regulators *YAP1* and *TAZ* to be inhibited in primed cells compared to unprimed cells at P1 (Figure 5E), but not at P3 or P5 (Supplemental Table 3). Specifically, 21 of 56 DEGs downstream of *YAP1* showed an inhibition of *YAP1* in primed cells (Figure 5F). Immunofluorescence imaging showed significantly greater YAP1 nuclear to cytoplasmic staining in unprimed cells than primed cells (Figure 5G), agreeing with our sequencing results that YAP was activated in unprimed cells.

Single-cell mechanics during expansion culture are dependent on both growth factor priming and passage number

Since YAP/TAZ activity corresponds to cytoskeletal tension, we sought to determine if growth factor priming during expansion culture causes detectable differences in chondrocyte mechanical properties using mechano-NPS (Figure 6). Unprimed cells were significantly larger than primed

cells at all three passages (Figure 6D). At P1, primed cells experienced greater deformations for an applied strain range than unprimed cells, suggesting that primed cells were less stiff ($p < 0.0001$; Figure 6E). No differences in cell stiffness were observed with priming at P3 ($p = 0.72$; Figure 6F) or P5 ($p = 0.05$; Supplemental Figure 4). There was a significant decrease in transverse deformation of primed cells between P1 and P3 ($p = 0.002$; Figure 6G); however, an increase in transverse deformation was observed between P3 and P5 ($p = 0.009$; Figure 6H). In contrast, no significant differences were seen in the transverse deformation of unprimed cells between P3 and P5 ($p = 0.65$; Figure 6I).

Priming during expansion culture improves development of functional engineered cartilage

Gross construct morphology revealed an increase in volume and tissue opacity compared to day 1 (Figure 7A). Constructs seeded with primed cells were ~15% smaller based on swelling ratio (Figure 7B). Both groups had similar proliferation rates in 3D culture (Figure 7C), suggesting that the increased proliferation rate in primed cells was limited to 2D culture. Constructs with primed cells produced tissue with greater GAG and collagen when normalized to DNA content (Figure 7D-7E) and wet weight (Figure 7F-7G) compared to the unprimed group. Greater matrix production was associated with a ~25% larger compressive modulus in the primed group (Figure 7H). Engineered tissue from both groups resulted in compressive mechanical properties (E_Y = 400-1000 kPa) and GAG content (native = 5-10 %w/w) within the range of native cartilage[22]. Total collagen content was consistent with previous cartilage tissue engineering studies (1.5-2%/ww), but significantly less than native values (native = 10-20 /%ww).

Discussion

Previous studies showed that chondrocyte dedifferentiation occurs during expansion culture and that additional biochemical cues, such as endogenous growth factors, are important for tissue

production[12, 13]. While many of these studies showed that priming cells with growth factors increases GAG and collagen production and *de novo* tissue stiffness, it is unknown how priming during 2D culture affects long-term cell response in 3D culture[14, 16, 23, 24]. Thus, we examined how growth factor priming with TGF-β1, PGDF-ββ, and FGF-2 alters cytoskeletal distribution, cell adhesion, single-cell mechanics, and gene expression to identify mechanisms by which cell behavior leads to improved tissue production. Our unbiased transcriptomic profiling and functional studies reveal that priming overrides mechanosensitive cytoskeletal remodeling during expansion culture, facilitating greater matrix production when cells are reintroduced to a 3D environment.

Cell adhesion is essential for cell function, and we found cell-substrate adhesion to be greater in unprimed cells at earlier passages (Figure 4). Like mesenchymal stem cells, dedifferentiated chondrocytes are known to adhere strongly to plastic in monolayer culture over successive passages; therefore, our results suggest that priming prevents dedifferentiation-associated cell adhesion[5]. Consistently, transcriptional analysis revealed that the gene ontology term "positive regulation of cell-substrate adhesion" was enriched in unprimed cells, and three of the most significant downregulated genes in primed cells were related to regulating cell-substrate adhesion (*APOA1, CDH13,* and *NID1).* Interestingly, all three genes have been related to OA,[25-27] with downregulation of *APOA1* in osteoarthritic cartilage and upregulation of *CDH13* expression in posttraumatic OA.

Vinculin imaging revealed development of focal adhesion complexes in unprimed cells, with fewer defined focal adhesions in primed cells until P3. Shin et al. showed an increase in focal adhesion area and length, and an upregulation of focal adhesion kinase with greater passages[28]. They also linked focal adhesion kinase expression to chondrocyte dedifferentiation, showing a loss of fibroblast characteristics and a recovery of collagen type II, aggrecan, and SOX9 expression

with focal adhesion kinase inhibition. While we did not observe downregulation of these genes with priming, our results agree with their findings that cell adhesion increased with passaging in unprimed cells, and the increase in cell-substrate adhesion could be delayed with priming.

Cell shape is indicative of chondrocyte phenotype and dedifferentiated chondrocytes have a flattened, fibroblastic morphology with actin polymerization and prominent actin stress fibers[10, 29-31]. An increase in actin polymerization has been linked to greater cell spreading area, while actin depolymerization results in chondrocyte redifferentiation[32, 33]. Interestingly, we found that priming preserved cell morphology, as noted by reduced cell spreading and fewer prominent F-actin fibers. At early passages, morphological characteristics of primed cells were similar to cells cultured on softer substrates with stiffnesses comparable to native cartilage. Specifically, primed cells at P1 and cells expanded on soft substrates have a smaller area, fewer stress fibers, and fewer focal adhesions compared to unprimed cells or cells cultured on stiff substrates[9, 11].

Cell mechanics depend on cytoskeleton structure and are important for regulating cell growth, adhesion, migration, and differentiation. Sliogeryte et al. showed that P1 chondrocytes are stiffer than freshly isolated chondrocytes,[34] and extensive research has shown a relationship between cell mechanics and substrate stiffness[35]. That is, cells adapt their cytoskeletal tension based on their microenvironment, leading to alterations in cell signaling[36]. Our findings showed that primed cells were less stiff than unprimed cells at P1, which agrees with previous work that showed an association between cell-substrate adhesion and cell stiffness[37, 38]. Generally, comparisons between unprimed and primed P1 cells were similar to previous observations between primary and passaged unprimed cells, including actin organization, focal adhesion, and cell spreading area[28, 33]. Moreover, by being less stiff, primed cells again showed similarities to cells cultured on softer

substrates[11]. Taken together, our findings suggest that priming may act to preserve primary chondrocyte mechanics.

A major finding in this study was the inhibition of YAP signaling in P1 primed cells. YAP and transcriptional co-activator TAZ are downstream effectors of the Hippo signaling pathway and play a major role in mechanotransduction. Additionally, YAP/ TAZ signaling has been linked to variations in chondrocyte phenotype in response to substrate stiffness, with chondrocytes cultured on softer substrates showing significantly less YAP nuclear localization and greater expression of Sox9, collagen type II, and aggrecan[39]. Zhang et al. found that human cartilage matrix stiffness increased with OA and that increasing matrix stiffness resulted in YAP activation with a gradual loss of chondrogenic phenotype[40]. Our results are consistent with these findings, where P1 unprimed cells showed YAP activation, and primed cells had many parallels to cells cultured on softer substrates, with downregulated YAP expression and decreased nuclear localization. Moreover, the relationship our results reveal between priming and YAP localization are consistent with other findings where cells lacking YAP displayed lower cell adhesion, stiffness, and contact area, and fewer actin bundles and stress fibers[37]. Since YAP mediates mechanical cues from the microenvironment, these results further support the notion that priming prevents cells from responding to the stiff monolayer culture.

Given the vast interactions of growth factors in cartilage development and homeostasis, it is likely that a combination of growth factors is required for regeneration[12]. The combination of TGF-β1, PGDF-ββ, and FGF-2 has been used to assess changes in chondrocyte proliferation, migration, and proteomics in 2D and 3D culture[14, 16, 23, 24]. To our knowledge the effect of this combination on cell mechanics, cell adhesion, and gene expression has not been investigated. This is important for understanding biomarkers that may predict preferred cartilage regeneration. Results from this

study were consistent with proteomic analysis of primed and unprimed canine chondrocytes, where proteins involved in synthesis and processing of ECM-components or associated with the cytoskeleton were downregulated in primed cells, while proteins associated with cell cycle regulation were upregulated[14].

Despite the findings of this manuscript, there are some important limitations. First, we cultured cells in hydrogel scaffolds following 5 passages. Future work should examine the relationship between cell properties and 3D tissue production during expansion culture at lower passages, where larger differences in cell behavior were observed. Second, gene expression analysis was only conducted on cells in 2D culture and 3D analysis only examined total glycosaminoglycan and collagen protein content. Further analysis on differences in 3D tissue growth would provide greater insight into long-term effects of priming during expansion culture.

In conclusion, our results show that growth factor priming during expansion culture alters chondrocyte phenotype, preventing them from remodeling their cytoskeleton in response to a stiff microenvironment. Specifically, priming delayed dedifferentiation associated changes in cell adhesion and cytoskeletal organization, with unprimed cells showing both a transcriptional and mechanistic increase in cell adhesion. The increase in cell adhesion was accompanied by an increase in focal adhesions, cell spreading area, stress fiber development, cell stiffness, and YAP1 activation. Furthermore, primed cells redifferentiated in 3D culture to produce *de novo* tissue with greater equilibrium modulus, GAG and total collagen content. Taken together, these results suggest that priming suppresses mechanobiological cytoskeletal remodeling to prevent chondrocyte dedifferentiation and to promote superior tissue formation. Future studies should investigate whether these observations are transferable to human cells, and if specific target genes

can be identified to reduce the cost associated with regenerating articular cartilage.

Acknowledgements: This work was supported by the National Institutes of Health National Institute of Arthritis and Musculoskeletal and Skin Diseases (NIH NIAMS R21 AR072248, GDO, LLS) and National Science Foundation Graduate Research Fellowship Program (EDL, KLC). We also thank UCSF genomics core for their assistance with RNA-seq analysis.

Contributions: EDL contributions include study design and ideation, data collection, data analysis, data interpretation, and writing; TW contributions include data collection, KLC contributions include mechano-NPS manufacturing and design, AG contributions include statistical study design and assessment; AAJ include study design and clinical translation; LLS contributed to study design, mechano-NPS design, data interpretation, and writing, TA contributed to study design, data analysis, data interpretation, and writing; GDO contributed to study design and ideation, data analysis, data interpretation, and writing. All authors contributed to editing the manuscript.

Role of funding source: The NIH provided funding to support personnel and laboratory supplies but did not play a role in the study design, data collection, data interpretation, or writing of this work.

Competing interest statement: There are no competing interests to disclose.

Declaration of generative AI in scientific writing: There is nothing to disclose.

References

1. Cisternas MG, Murphy L, Sacks JJ, Solomon DH, Pasta DJ, Helmick CG. Alternative Methods for Defining Osteoarthritis and the Impact on Estimating Prevalence in a US Population-Based Survey. Arthritis Care Res (Hoboken) 2016; 68: 574-580.
2. Culliford D, Maskell J, Judge A, Cooper C, Prieto-Alhambra D, Arden NK, et al. Future projections of total hip and knee arthroplasty in the UK: results from the UK Clinical Practice Research Datalink. Osteoarthritis Cartilage 2015; 23: 594-600.
3. Zhao Z, Fan C, Chen F, Sun Y, Xia Y, Ji A, et al. Progress in Articular Cartilage Tissue Engineering: A Review on Therapeutic Cells and Macromolecular Scaffolds. Macromol Biosci 2020; 20: e1900278.
4. Ebert JR, Fallon M, Wood DJ, Janes GC. Long-term Prospective Clinical and Magnetic Resonance Imaging-Based Evaluation of Matrix-Induced Autologous Chondrocyte Implantation. Am J Sports Med 2021; 49: 579-587.
5. Charlier E, Deroyer C, Ciregia F, Malaise O, Neuville S, Plener Z, et al. Chondrocyte dedifferentiation and osteoarthritis (OA). Biochem Pharmacol 2019; 165: 49-65.
6. Bianchi VJ, Lee A, Anderson J, Parreno J, Theodoropoulos J, Backstein D, et al. Redifferentiated Chondrocytes in Fibrin Gel for the Repair of Articular Cartilage Lesions. Am J Sports Med 2019; 47: 2348-2359.
7. Duan L, Ma B, Liang Y, Chen J, Zhu W, Li M, et al. Cytokine networking of chondrocyte dedifferentiation in vitro and its implications for cell-based cartilage therapy. Am J Transl Res 2015; 7: 194-208.
8. von der Mark K, Gauss V, von der Mark H, Muller P. Relationship between cell shape and type of collagen synthesised as chondrocytes lose their cartilage phenotype in culture. Nature 1977; 267: 531-532.
9. Genes NG, Rowley JA, Mooney DJ, Bonassar LJ. Effect of substrate mechanics on chondrocyte adhesion to modified alginate surfaces. Arch Biochem Biophys 2004; 422: 161-167.
10. Schuh E, Kramer J, Rohwedel J, Notbohm H, Muller R, Gutsmann T, et al. Effect of matrix elasticity on the maintenance of the chondrogenic phenotype. Tissue Eng Part A 2010; 16: 1281-1290.
11. Zhang Q, Yu Y, Zhao H. The effect of matrix stiffness on biomechanical properties of chondrocytes. Acta Biochim Biophys Sin (Shanghai) 2016; 48: 958-965.
12. Fortier LA, Barker JU, Strauss EJ, McCarrel TM, Cole BJ. The role of growth factors in cartilage repair. Clin Orthop Relat Res 2011; 469: 2706-2715.
13. van der Kraan PM, Buma P, van Kuppevelt T, van den Berg WB. Interaction of chondrocytes, extracellular matrix and growth factors: relevance for articular cartilage tissue engineering. Osteoarthritis Cartilage 2002; 10: 631-637.
14. Alegre-Aguaron E, Sampat SR, Xiong JC, Colligan RM, Bulinski JC, Cook JL, et al. Growth factor priming differentially modulates components of the extracellular matrix proteome in chondrocytes and synovium-derived stem cells. PLoS One 2014; 9: e88053.
15. Cigan AD, Roach BL, Nims RJ, Tan AR, Albro MB, Stoker AM, et al. High seeding density of human chondrocytes in agarose produces tissue-engineered cartilage approaching native mechanical and biochemical properties. J Biomech 2016; 49: 1909-1917.
16. Barbero A, Grogan S, Schafer D, Heberer M, Mainil-Varlet P, Martin I. Age related changes in human articular chondrocyte yield, proliferation and post-expansion chondrogenic capacity. Osteoarthritis Cartilage 2004; 12: 476-484.
17. O'Connell GD, Tan AR, Cui V, Bulinski JC, Cook JL, Attur M, et al. Human chondrocyte migration behaviour to guide the development of engineered cartilage. J Tissue Eng Regen Med 2017; 11: 877-886.

18. Kim J, Han S, Lei A, Miyano M, Bloom J, Srivastava V, et al. Characterizing cellular mechanical phenotypes with mechano-node-pore sensing. Microsyst Nanoeng 2018; 4.
19. Loffek S, Hurskainen T, Jackow J, Sigloch FC, Schilling O, Tasanen K, et al. Transmembrane collagen XVII modulates integrin dependent keratinocyte migration via PI3K/Rac1 signaling. PLoS One 2014; 9: e87263.
20. Kim M, Farrell MJ, Steinberg DR, Burdick JA, Mauck RL. Enhanced nutrient transport improves the depth-dependent properties of tri-layered engineered cartilage constructs with zonal co-culture of chondrocytes and MSCs. Acta Biomater 2017; 58: 1-11.
21. Bosnakovski D, Mizuno M, Kim G, Takagi S, Okumura M, Fujinaga T. Chondrogenic differentiation of bovine bone marrow mesenchymal stem cells (MSCs) in different hydrogels: influence of collagen type II extracellular matrix on MSC chondrogenesis. Biotechnol Bioeng 2006; 93: 1152-1163.
22. Nguyen AM, Levenston ME. Comparison of osmotic swelling influences on meniscal fibrocartilage and articular cartilage tissue mechanics in compression and shear. J Orthop Res 2012; 30: 95-102.
23. Francioli SE, Martin I, Sie CP, Hagg R, Tommasini R, Candrian C, et al. Growth factors for clinical-scale expansion of human articular chondrocytes: relevance for automated bioreactor systems. Tissue Eng 2007; 13: 1227-1234.
24. Sampat SR, O'Connell GD, Fong JV, Alegre-Aguaron E, Ateshian GA, Hung CT. Growth factor priming of synovium-derived stem cells for cartilage tissue engineering. Tissue Eng Part A 2011; 17: 2259-2265.
25. Tsezou A, Iliopoulos D, Malizos KN, Simopoulou T. Impaired expression of genes regulating cholesterol efflux in human osteoarthritic chondrocytes. J Orthop Res 2010; 28: 1033-1039.
26. Liu CC, Lee HC, Peng YS, Tseng AH, Wu JL, Tsai WY, et al. Transcriptome Analysis Reveals Novel Genes Associated with Cartilage Degeneration in Posttraumatic Osteoarthritis Progression. Cartilage 2021; 13: 1249S-1262S.
27. Cui S, Zhang X, Hai S, Lu H, Chen Y, Li C, et al. Molecular mechanisms of osteoarthritis using gene microarrays. Acta Histochem 2015; 117: 62-68.
28. Shin H, Lee MN, Choung JS, Kim S, Choi BH, Noh M, et al. Focal Adhesion Assembly Induces Phenotypic Changes and Dedifferentiation in Chondrocytes. J Cell Physiol 2016; 231: 1822-1831.
29. Glowacki J, Trepman E, Folkman J. Cell shape and phenotypic expression in chondrocytes. Proc Soc Exp Biol Med 1983; 172: 93-98.
30. Lauer JC, Selig M, Hart ML, Kurz B, Rolauffs B. Articular Chondrocyte Phenotype Regulation through the Cytoskeleton and the Signaling Processes That Originate from or Converge on the Cytoskeleton: Towards a Novel Understanding of the Intersection between Actin Dynamics and Chondrogenic Function. Int J Mol Sci 2021; 22.
31. Zwicky R, Baici A. Cytoskeletal architecture and cathepsin B trafficking in human articular chondrocytes. Histochem Cell Biol 2000; 114: 363-372.
32. Brown PD, Benya PD. Alterations in chondrocyte cytoskeletal architecture during phenotypic modulation by retinoic acid and dihydrocytochalasin B-induced reexpression. J Cell Biol 1988; 106: 171-179.
33. Parreno J, Nabavi Niaki M, Andrejevic K, Jiang A, Wu PH, Kandel RA. Interplay between cytoskeletal polymerization and the chondrogenic phenotype in chondrocytes passaged in monolayer culture. J Anat 2017; 230: 234-248.
34. Sliogeryte K, Botto L, Lee DA, Knight MM. Chondrocyte dedifferentiation increases cell stiffness by strengthening membrane-actin adhesion. Osteoarthritis Cartilage 2016; 24: 912-920.
35. Discher DE, Janmey P, Wang YL. Tissue cells feel and respond to the stiffness of their substrate. Science 2005; 310: 1139-1143.
36. Ingber DE. Tensegrity I. Cell structure and hierarchical systems biology. J Cell Sci 2003; 116: 1157-1173.

37. Nardone G, Oliver-De La Cruz J, Vrbsky J, Martini C, Pribyl J, Skladal P, et al. YAP regulates cell mechanics by controlling focal adhesion assembly. Nat Commun 2017; 8: 15321.
38. Sen S, Kumar S. Cell-Matrix De-Adhesion Dynamics Reflect Contractile Mechanics. Cell Mol Bioeng 2009; 2: 218-230.
39. Zhong W, Li Y, Li L, Zhang W, Wang S, Zheng X. YAP-mediated regulation of the chondrogenic phenotype in response to matrix elasticity. J Mol Histol 2013; 44: 587-595.
40. Zhang X, Cai D, Zhou F, Yu J, Wu X, Yu D, et al. Targeting downstream subcellular YAP activity as a function of matrix stiffness with Verteporfin-encapsulated chitosan microsphere attenuates osteoarthritis. Biomaterials 2020; 232: 119724.

1 **Illustrations and Tables**

2 # Figures

3 ***Figure 1***. *Schematic of study design for chondrocytes primed (+GF) or unprimed (-GF) with a*
4 *growth factor cocktail during expansion culture. Gene expression (RNA-seq and qPCR), cell*
5 *morphology and cytoskeletal protein distribution (IF), cell mechanics (mechano-NPS), and cell*
6 *adhesion (centrifugation-based and trypsin-based assay) were assessed following passages 1, 3,*
7 *and 5. Following passage 5, cells were embedded into agarose hydrogels, and mechanical and*
8 *biochemical properties were assessed at day 35.*

9 ***Figure 2.*** *Unbiased RNA-sequencing results for primed and unprimed chondrocytes during 2D*
10 *expansion culture through five passages. Culture media for primed chondrocytes was*
11 *supplemented with a growth factor cocktail. (**A**) Heat map of z-scores show gene expression*
12 *patterns for differentially expressed genes (DEGs) based on priming for each passage; blue*
13 *indicates downregulated genes and red indicates upregulated genes. Columns represent samples*
14 *and rows represent genes. (**B**) Principal component analysis shows the separation of samples*
15 *based on priming and passage (n=3 per group). (**C**) Number of down and upregulated DEGs at*
16 *each passage (FDR <0.01). (**D**) Venn diagram showing number of common and unique DEGs*
17 *based on passage. Top ten down- (**E**) and up-regulated (**F**) genes based on false discovery rate*
18 *(FDR) in primed cells relative to unprimed cells at each passage. Log2(fold change) values for*
19 *each gene displayed at each passage in columns and FDR values displayed below each table. (**G**)*
20 *Comparison of results from four genes measured using both RT-qPCR and RNAseq to validate*
21 *results from RNAseq. Results from RT-qPCR are shown as mean ± standard deviation (n=3).*
22 *mRNA ratio of collagen type II to collagen type I (**H**) and aggrecan to veriscan (**I**) in unprimed*
23 *and primed cells at each passage (n=3 per group, mean ± SD). Statistical analysis was performed*

using a two-way ANOVA (factors = passage and treatment) with Tukey-Kramer post-hoc test. A represents statistical difference based on priming at each passage. B represents statistical difference compared to passage 1, for primed cells. C represents statistical difference compared to passage 1, for unprimed cells.

Figure 3. *Gene ontology (GO) enrichment analysis of differentially expressed genes based on priming for passages 1, 3, and 5 (P1, P3, and P5) identified using DAVID functional enrichment tool. Dot plots show biological processes and cellular components downregulated* ***(A, B)*** *and upregulated* ***(C, D)*** *in primed cells compared to unprimed cells. Top 10 significantly enriched GO terms with -log Benjamini–Hochberg adjusted p-value < 0.05 are shown. Gene ratio represents the ratio of the genes belonging to the gene ontology term to the total number of down or upregulated DEGs at that passage. Colored labels on y-axis represent grouping for clarity. Reg. = regulation.*

Figure 4. Effect of growth factor priming on cell adhesion*.* ***(A)*** *Heat map showing z-scores of significantly expressed DEGs identified as part of the gene ontology term "positive regulation of cell substrate adhesion" (Supplemental Table 2).* ***(B)*** *Centrifugation-based assay results (n=3 wells/group; 9 images/well). Statistical analysis was performed using a two-way ANOVA, with factors passage and growth factor treatment, and a Tukey's multiple comparisons post hoc test. Groups were compared based on growth factor priming at each passage (*p<0.0001 for connected groups). A Trypsin-based assay was performed to evaluate differences in cell detachment based on priming at* ***(C)*** *passage 1 and* ***(D)*** *3 (n =3 wells/group; 3 images/well). Statistical analysis was performed using a two-way ANOVA, with factors passage and culture time, followed by a Tukey's multiple comparisons test. Groups were compared based on growth factor priming at each time point, *p<0.02. The trypsin-based assay was used to compared differences in cell detachment*

*between passage 1 and 3 for **(E)** unprimed and **(F)** primed cells (two-way ANOVA factors = passage and time; Tukey's multiple comparisons post-hoc, n=3 wells/group; 3 images/well) Groups were compared based on passage number at each time point, *p<0.0001. Grey lines indicate mean ± standard deviation (SD).*

***Figure 5:** Growth factor priming influences stress fiber development, cell spreading, and YAP1 signaling at passage 1. **(A)** Visual representation of immunofluorescent staining of F-actin and vinculin in primed and unprimed cells 48 hour following plating and passage 1, 3 and 5. Images of passage 1 cells are selected with a grey box to highlight differences. Scale bar:10 m. Differences in **(B)** percent of cells with stress fibers (n=3 wells/ group; 52-79 total cells/group) and **(C)** cell spreading area (n=3 wells/ group; 45-80 total cells/group) based on priming were found using phalloidin stained cells at passage 1, 3, and 5. Two-way ANOVA, factors= passage and growth factor priming, followed by Tukey's multiple comparisons tests. Groups connected by the same letter are not statistically different. **(D)** Diseases and biological functions identified by IPA Downstream Effects Analysis that are associated with DEGs in primed cells compared to unprimed cells. Activation z-scores shown for each category, blue (negative z-score) indicates the biological diseases is decreased in primed cells compared to unprimed (z-2 is a statistically significant decrease). All groups displayed have -log(p-value)>13.2, calculated by IPA using right-tailed Fishers Exact test. **(E)** IPA Upstream Regulators tool predicted expression of YAP1 and TAZ based on DEGs in primed cells compare to unprimed cells (z-2 is inhibited). P-value calculate using right-tailed Fishers Exact test. **(F)** Target molecules in dataset in support of inhibition of YAP1 expression in passage 1 (P1) primed cells compared to unprimed. Blue (downregulated) and pink (upregulated) are the log2FC expressions of the gene in the data set. Grey scale shading represents the predicated measurement direction of YAP1 based on the measurement direction of that gene*

(inhibited, activated, or affected). For genes labeled affected, literature suggests the genes are regulated by YAP1, but it is unknown if the gene is upregulated or downregulated by YAP1 expression. ***(G)****Representative images of YAP1 and nucleus immunostaining of cells at passage 1. Scale bar:10 m.****(H)*** *Quantification of nuclear to cytoplasm staining intensity of YAP1 based on priming in P1 cells (n=3 wells/group; 297 total cells/group). Statistical analysis was performed using an unpaired two tailed parametric t-test, p=0.006.*

Figure 6: *Influence of growth factor priming on chondrocyte mechanics during monolayer expansion.* ***(A)*** *Schematic representation of mechano-NPS microfluidic device used to measure cell mechanics, including a series of node-pore segments where free cell diameter is calculated and a contraction channel where cells experience a constant strain.* ***(B)*** *Cross-sectional view of a node-pore segment and the contraction channel occupied by a cell (red circle).* w_{pore}, w_{node}, w_{cont}, *and* $h_{channel}$ *correspond to the widths of the pores, nodes, contraction channel, and the channel height, respectively. For the devices used,* $w_{pore} = 18$, $w_{node}=24$, $w_{cont}= 9.8$ *or* 10.5 *, and* $h_{channel} =16.6$ *or* 16.67 *.* ***(C)*** *Expected current pulses as a cell transits the device. I,* ΔI_{np}, *and* $\Delta I_{c,}$ *correspond to the baseline current and the current drops in the node-pore and contraction channel segments.* ΔT_c *corresponds to the cell's transit time in the contraction channel. Figure adapted from* [18]*.* ***(D)*** *Cell diameter measured using mNPS in preliminary experiments to determine appropriate contraction channel sizes that maintained a consistent strain range (n=114, two- way ANOVA, factors= passage and growth factor priming, followed by Tukey's multiple comparisons tests. Groups connected by the same letter are not statistically different). Deformed diameter verse strain for* ***(E)*** *passage 1 (n=109 cells/group) and* ***(F)*** *passage 3 (n=115 cells/group) cells based on priming. Line of best fit (linear) displayed for clarity. Differences in transverse deformation based on passage number for primed cells at* ***(G)*** *P1 and P3 (n=68 cells/ group; applied strain = 0.15- 0.39) and at* ***(H)*** *P3 and P5 (n=117cells/group; applied strain = 0.1- 0.34)* ***(I)*** *Comparison of transverse deformation in unprimed cells based on passaging at P3 and P5 (n=262 cells/group; applied strain = 0.1- 0.35). At least 3 microfluidics devices were used for each group in all experiments. For statistical analysis of results from mechano-NPS* ***(E-I)****, 1-1 matching*

with a caliper of 0.1 was used to ensure no significant differences between groups based on strain and then a two-sided permutation test was used to calculate p-values (see methods for information on test statistics).

Figure 7: *Engineered tissue production of constructs primed and unprimed during expansion culture at day 35.* ***(A)*** *Representative images of constructs containing cells primed during expansion culture at day 1 and 35 and a construct containing unprimed cells at day 35.* ***(B)*** *Swelling ratio, defined as day 35 wet weight normalized to average wet weight at day 1 for each group, for constructs containing cells primed and unprimed during expansion culture.* ***(C)*** *The number of cells/ constructs measured weekly for the 5-week culture period (n=6-8 constructs/ group; two-way ANOVA, factor= growth factor priming and days of culture, followed by Tukey's multiple comparisons post-hoc). Groups connected by the same letter are not statistically different. GAG and collagen content normalized by DNA content* ***(D, E)*** *and wet weight* ***(F, G)****, respectively, for constructs with cells primed and unprimed during expansion (Day 35 values).* ***(H)*** *Equilibrium Young's modulus for constructs at day 35. (****B, D-H****) Statistics were calculated using a two-tailed parametric t-test (n=8 constructs/ group, mean ± SD). **p<0.01, ***p<0.001, ****p<0.0001.*

Supplemental Figures

Supplemental *Figure 1:* *Representative images of cells classified as (A) cells with no defined stress fibers in the cytoplasm and (B) cells with clearly defined stress fibers. Scale bar is 10 m.*

Supplemental Figure 2: *Representative image of engineered cartilage constructs seeded with primed cells at passage 3. The restriction of nutrient diffusion resulted in unreliable mechanical testing data. The scale bar is 1mm.*

Supplemental Figure 3. *Molecule function gene ontology terms identified in growth factor primed cells compared to unprimed cells at passage 1, 3, and 5. Top 10 most significant GO terms from each passage with a -log Benjamini–Hochberg adjusted p-value < 0.05 are shown. Gene ratio represents the ratio of the genes belonging to the gene ontology term to the total number of down or upregulated DEGs at that passage.*

Supplemental Figure 4*: Deformed diameter verse strain for passage 5 primed and unprimed cells (n=3 microfluidic devices/group; 152 cells/group). The linear line of best fit is displayed for clarity. For statistical analysis, 1-1 matching with a caliper of 0.1 was used to ensure no significant differences between groups based on strain and then a two-sided permutation test was used to calculate p-values (see methods for information on test statistics).*

Supplemental Table 1: *Primer sequences for genes used in qPCR*[21].

Supplemental Table 2: *Significant gene ontology terms identified by DAVID that are related to cell adhesion in DEG based on priming at passage 1, 3, and 5. All terms shown are downregulated in primed cells compared to unprimed unless they contain (+GF) in the column labeled passage. Count represents the number of DEGs belonging to that gene ontology term. Percent represents the ratio of the genes belonging to the gene ontology term to the total number of down or upregulated DEGs at that passage. Benjamini–Hochberg adjusted p-value < 0.05.*

Supplemental Table 3: *IPA predicted expression of YAP1 and TAZ as upstream regulators based on DEGs in primed compared to unprimed cells at P3 and P5. Z-score -2 is predicted to be significantly inhibited and z-score 2 is predicted to be significantly activated. P-values were calculated with a right-tailed Fisher's Exact test and the number of target molecules in the data set identified by IPA is presented. The significance and expression of both genes in the experimental data set are included (RNA-sequencing columns).*

Figure 1

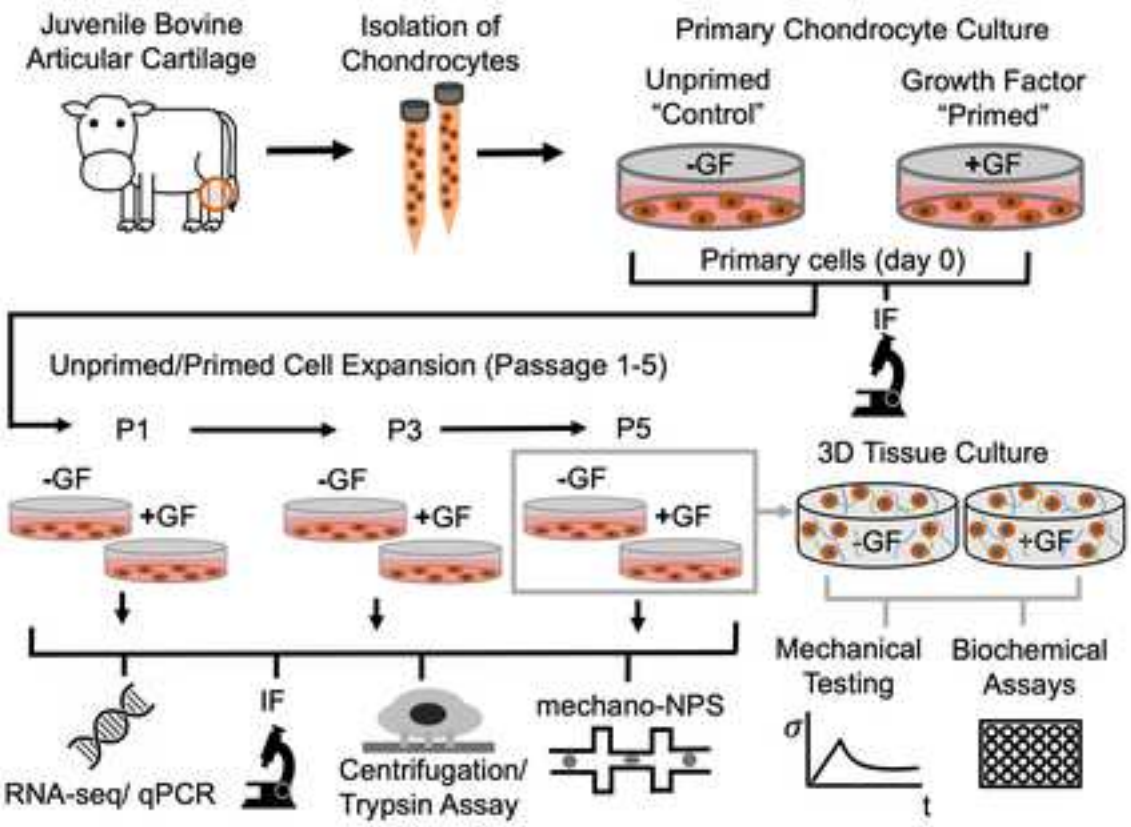

Figure 2

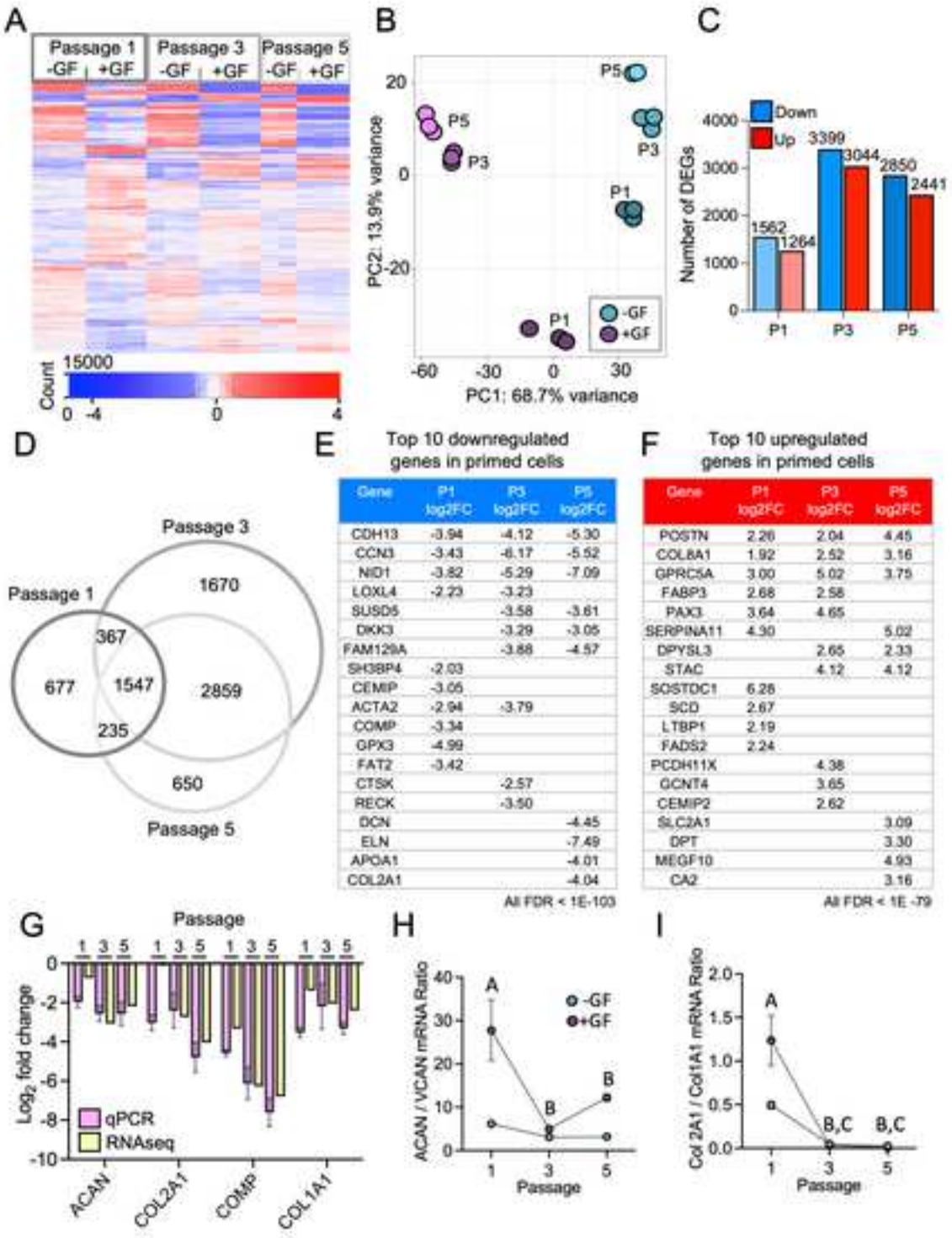

Figure 3

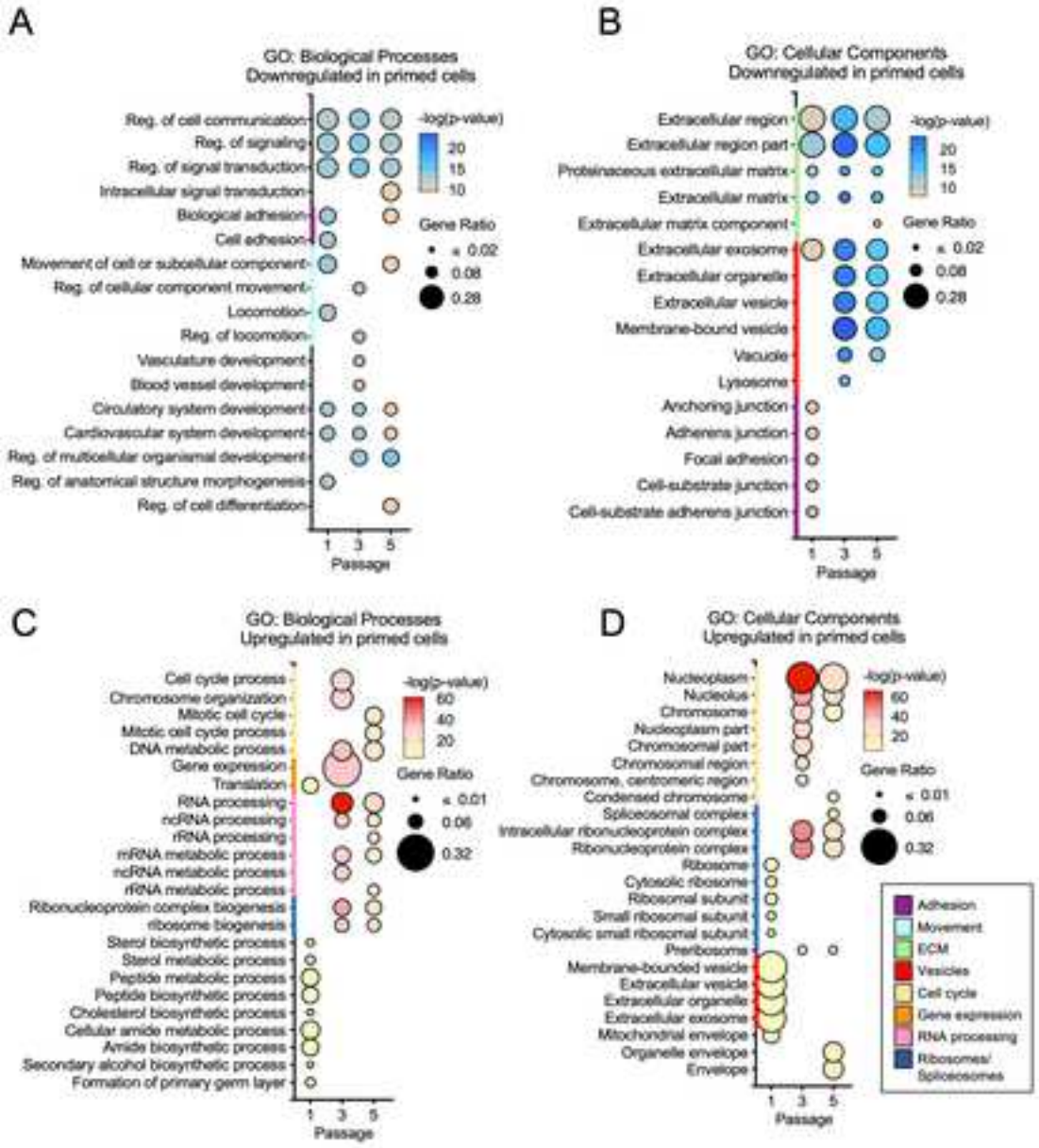

Figure 4

Click here to access/download;Figure;Figure4.tiff

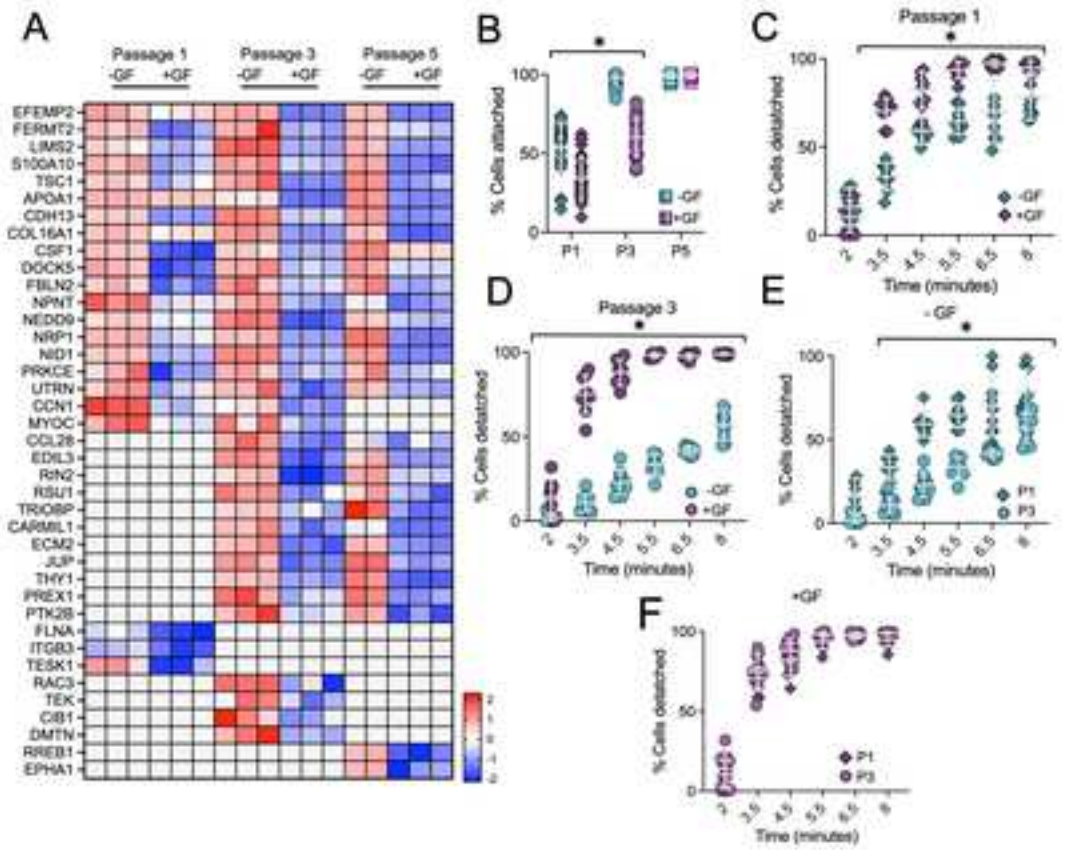

Figure 5

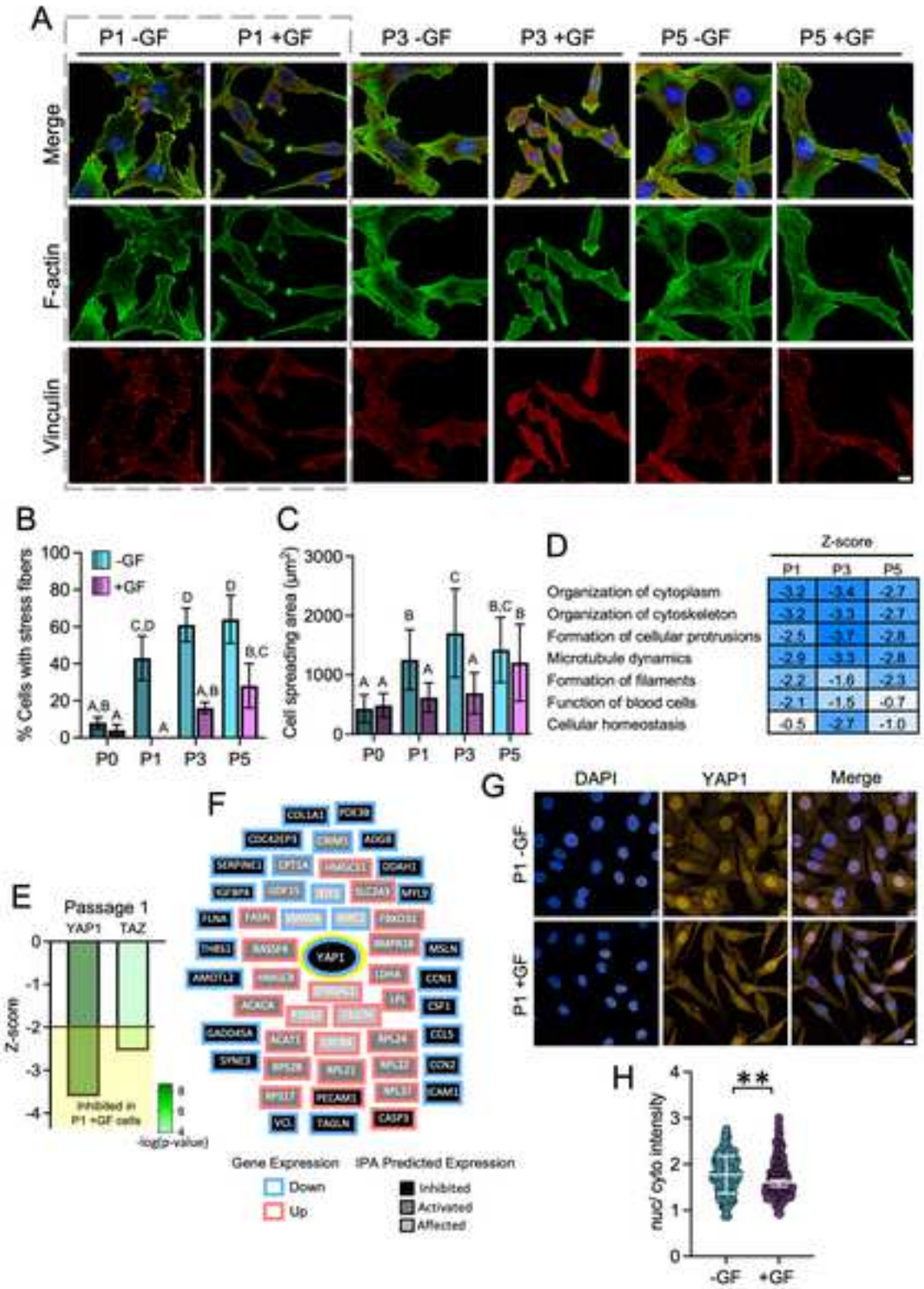

Figure 6

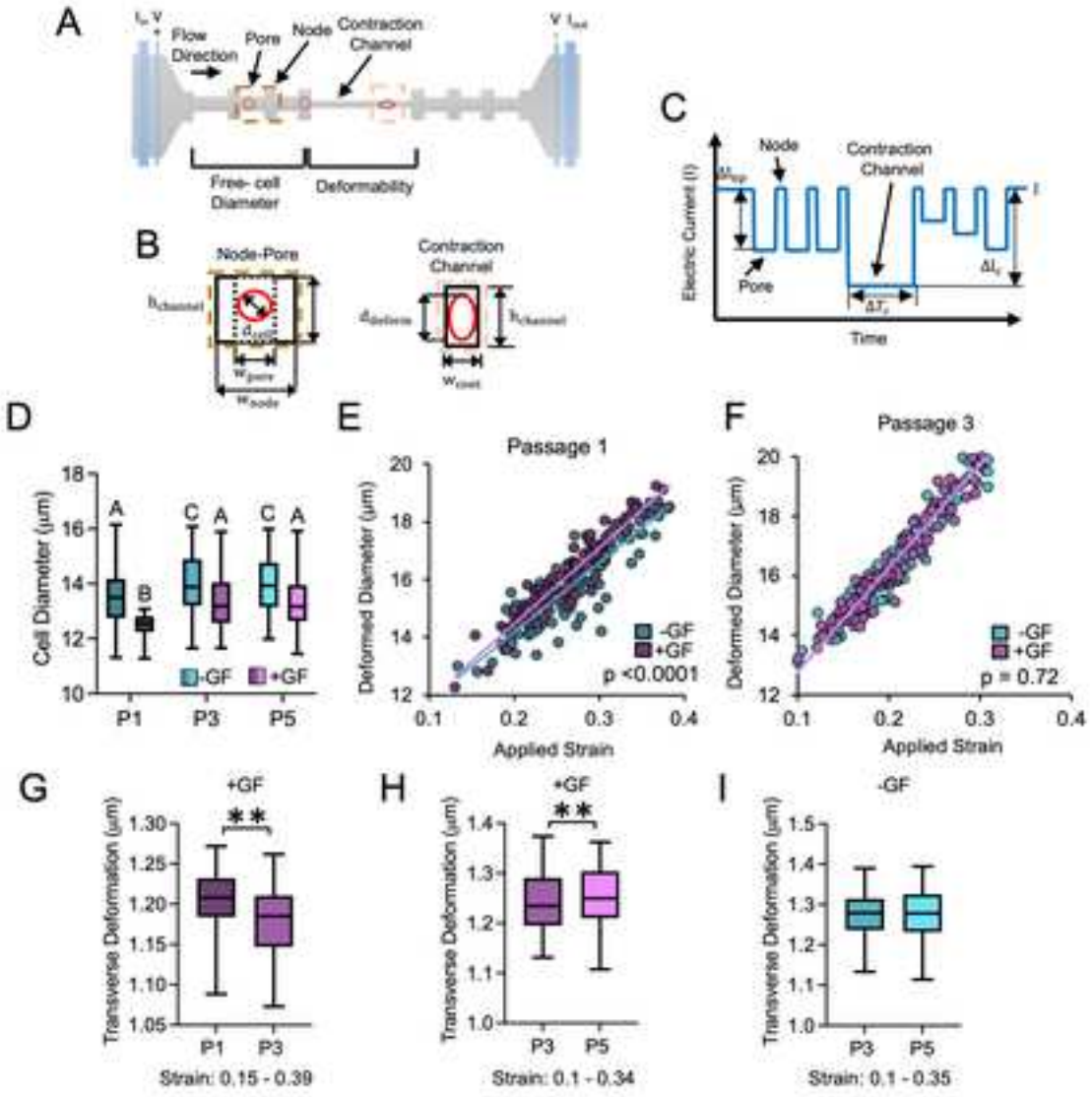

OSTEOARTHRITIS AND CARTILAGE

AUTHORS' DISCLOSURE

Manuscript title __*Priming chondrocytes during expansion culture alters cell behaviour and improves matrix production in 3D culture*

Corresponding author ____Grace O'Connell, PhD_____

Authorship
All authors should have made substantial contributions to all of the following: (1) the conception and design of the study, or acquisition of data, or analysis and interpretation of data, (2) drafting the article or revising it critically for important intellectual content, (3) final approval of the version to be submitted. By signing below each author also verifies that he (she) confirms that neither this manuscript, nor one with substantially similar content, has been submitted, accepted or published elsewhere (except as an abstract). Each manuscript must be accompanied by a declaration of contributions relating to sections (1), (2) and (3) above. This declaration should also name one or more authors who take responsibility for the integrity of the work as a whole, from inception to finished article. These declarations will be included in the published manuscript.

Acknowledgement of other contributors
All contributors who do not meet the criteria for authorship as defined above should be listed in an acknowledgements section. Examples of those who might be acknowledged include a person who provided purely technical help, writing assistance, or a department chair who provided only general support. Such contributors must give their consent to being named. Authors should disclose whether they had any writing assistance and identify the entity that paid for this assistance.

Conflict of interest
At the end of the text, under a subheading "Conflict of interest statement" all authors must disclose any financial and personal relationships with other people or organisations that could inappropriately influence (bias) their work. Examples of potential conflicts of interest include employment, consultancies, stock ownership, honoraria, paid expert testimony, patent applications/registrations, and research grants or other funding.

Declaration of Funding
All sources of funding should be declared as an acknowledgement at the end of the text.

Role of the funding source
Authors should declare the role of study sponsors, if any, in the study design, in the collection, analysis and interpretation of data; in the writing of the manuscript; and in the decision to submit the manuscript for publication. If the study sponsors had no such involvement, the authors should state this.

Studies involving humans or animals
Clinical trials or other experimentation on humans must be in accordance with the ethical standards of the responsible committee on human experimentation (institutional and national) *and* with the Helsinki Declaration of 1975, as revised in 2000. Randomized controlled trials should follow the Consolidated Standards of

Reporting Trials (CONSORT) guidelines and be registered in a public trials registry.

Studies involving experiments with animals were in accordance with institution guidelines

Please sign below to certify your manuscript complies with the above requirements and then upload this form at https://www.editorialmanager.com/oac/

Author	**Signature**	**Date**
Emily Lindberg	DocuSigned by: Emily Lindberg A960341C8FBE430...	6/25/2023
Tiffany Wu	DocuSigned by: 16765423E97B43A...	6/23/2023
Kristen Cotner	DocuSigned by: Kristen Cotner 1795A6EC631F4EF...	6/25/2023
Amanda Glazer	DocuSigned by: Amanda Glazer 7D38D1910875487...	6/25/2023
Amir A. Jamali	DocuSigned by: Amir A. Jamali B4E4B79699B64A2...	6/24/2023
Lydia Sohn	DocuSigned by: Lydia Sohn E2F549280FE5491...	6/24/2023
Tamara Alliston	DocuSigned by: Tamara Alliston E233CABEF261499...	6/28/2023
Grace D. O'Connell	DocuSigned by: Grace O'Connell 9F3C0FF166E14FF...	6/23/2023